JACS
JOURNAL OF THE AMERICAN CHEMICAL SOCIETY
Article
pubs.acs.org/JACS

# The Role of Phosphate in a Multistep Enzymatic Reaction: Reactions of the Substrate and Intermediate in Pieces

Svetlana A. Kholodar,[†] C. Leigh Allen,[‡] Andrew M. Gulick,[‡] and Andrew S. Murkin*[,†]

[†]Department of Chemistry, University at Buffalo, Buffalo, New York 14260-3000, United States

[‡]Hauptman-Woodward Institute and Department of Structural Biology, University at Buffalo, Buffalo, New York 14203-1102, United States

Supporting Information

**ABSTRACT:** Several mechanistically unrelated enzymes utilize the binding energy of their substrate's nonreacting phosphoryl group to accelerate catalysis. Evidence for the involvement of the phosphodianion in transition state formation has come from reactions of the substrate in pieces, in which reaction of a truncated substrate lacking its phosphorylmethyl group is activated by inorganic phosphite. What has remained unknown until now is how the phosphodianion group influences the reaction energetics at different points along the reaction coordinate. 1-Deoxy-D-xylulose-5-phosphate (DXP) reductoisomerase (DXR), which catalyzes the isomerization of DXP to 2-C-methyl-D-erythrose 4-phosphate (MEsP) and subsequent NADPH-dependent reduction, presents a unique opportunity to address this concern. Previously, we have reported the effect of covalently linked phosphate on the energetics of DXP turnover. Through the use of chemically synthesized MEsP and its phosphate-truncated analogue, 2-C-methyl-D-glyceraldehyde, the current study revealed a loss of 6.1 kcal/mol of kinetic barrier stabilization upon truncation, of which 4.4 kcal/mol was regained in the presence of phosphite dianion. The activating effect of phosphite was accompanied by apparent tightening of its interactions within the active site at the intermediate stage of the reaction, suggesting a role of the phosphodianion in disfavoring intermediate release and in modulation of the on-enzyme isomerization equilibrium. The results of kinetic isotope effect and structural studies indicate rate limitation by physical steps when the covalent linkage is severed. These striking differences in the energetics of the natural reaction and the reactions in pieces provide a deeper insight into the contribution of enzyme−phosphodianion interactions to the reaction coordinate.

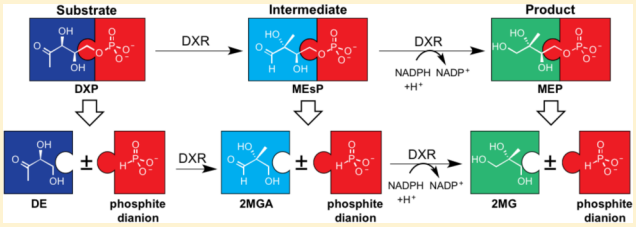


## INTRODUCTION

Phosphorylated biomolecules play a central role in metabolism of all living species. The phosphate group as a part of a small molecule is often nonreacting but essential for the recognition and catalysis by enzymes. Previous studies by Richard and co-workers have demonstrated that mechanistically unrelated enzymes including triosephosphate isomerase (TIM),[6−8] orotidine-5′-monophosphate decarboxylase (OMPDC),[10] and glycerol-3-phosphate dehydrogenase (GPDH)[11] can bind and turnover truncated versions of their corresponding substrates lacking the terminal phosphorylmethyl group with catalytic efficiencies decreased dramatically by factors of $10^8$−$10^{10}$. These reactions could be rescued by factors of up to 80 000 by the inclusion of inorganic phosphite dianion. These curious results have been the subject of several reviews[8,12−14] and have been rationalized with respect to the classical paradigm introduced by Jencks,[15] in which binding interactions between a nonreacting determinant of the substrate and the active site serve a significant role in transition state stabilization. Specifically, this binding energy is argued to drive thermodynamically unfavorable conformational changes that pre-organize the enzyme's active site for catalysis. In agreement, structural data suggest that phosphodianion binding in the active site serves as a trigger for closure of the flexible loop over the active site of each of these phosphite-activated enzymes.[13] This critical conformational change is implicated in sequestration of the active site from bulk solvent, thus creating a lower dielectric environment poised for catalysis.

In earlier work we probed the generality of phosphodianion-assisted catalysis by extending the approach to 1-deoxy-D-xylulose-5-phosphate (DXP) reductoisomerase (DXR),[16] an enzyme with significantly different characteristics from those described above. DXR performs a multistep reaction that proceeds through retro-aldol/aldol isomerization of the ketone DXP to the branched aldehyde intermediate 2-C-methyl-D-erythrose 4-phosphate (MEsP), followed by NADPH-dependent reduction to form 2-C-methyl-D-erythritol 4-phosphate (MEP) (Scheme 1).[17] Importantly, a phosphodianion group is critical for substrate turnover[18,19] and for inhibition by the antibiotics fosmidomycin and FR-900098. In our previous study, we demonstrated that 1-deoxy-L-erythrulose (DE), a DXP analogue lacking the terminal phosphorylmethyl group, can be converted by *Mycobacterium tuberculosis* DXR (*Mt*DXR)

**Received:** December 23, 2014
**Published:** February 2, 2015





DOI: 10.1021/ja512911f
J. Am. Chem. Soc. 2015, 137, 2748−2756

**Scheme 1. Mechanism for DXR-Catalyzed Conversion of DXP to MEP and DE to 2MG**

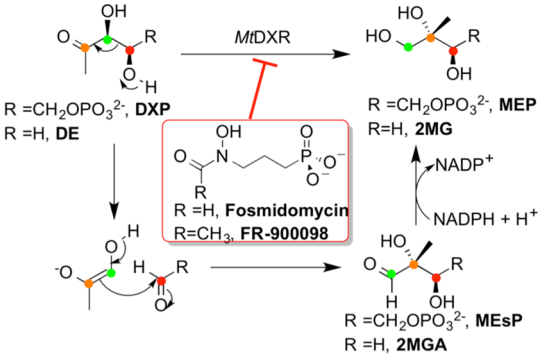


to the corresponding MEP analogue 2-*C*-methylglycerol (2MG) with a $k_{cat}/K_m$ that is $10^6$ lower than that for DXP.[16] As with the enzymes mentioned above, phosphite dianion was found to be a non-essential activator; however, only a 5-fold increase in $k_{cat}/K_m$ and $k_{cat}$ was observed at saturating concentrations. This low activation factor can be rationalized by (1) the much lower catalytic efficiency of *Mt*DXR, suggestive of intrinsically suboptimal transition state stabilization by the phosphodianion, (2) the distribution of total binding energy between distal portions of the substrate (i.e., the phosphodianion at C-5 and the divalent metal-binding groups at C-2 and C-3), and (3) the multistep nature of the reaction, in which the degree of transition state stabilization by the phosphodianion may vary along the reaction coordinate.

In this work we report a complete investigation of the role of the covalent linkage to the phosphodianion in modulation of the energy landscape of the *Mt*DXR-catalyzed reaction. The reaction intermediate MEsP and its truncated version, 2-*C*-methyl-D-glyceraldehyde (2MGA), were synthesized and kinetically characterized to reveal a possible role of the phosphodianion in reducing of the energy gap between enzyme-bound substrate and intermediate. On the basis of X-ray structural data and kinetic isotope effects (KIEs) for the natural compounds and their corresponding "pieces", we suggest a function of the covalently linked phosphodianion in the productive orientation of the substrate and intermediate in the catalytic site and/or in induction of conformational changes required for catalysis.

## EXPERIMENTAL PROCEDURES

**Materials.** All chemicals were of analytical or reagent grade and were used without further purification unless otherwise stated. *Escherichia coli* DXP synthase (DXS) was expressed and purified as reported.[20] *Mt*DXR was cloned, expressed, purified, and quantified as reported previously.[21] *Pichia pastoris* alcohol oxidase was purchased from MP Biomedicals. Bacterial glucose dehydrogenase was from Toyobo. Bovine liver catalase was from Calbiochem. ($^2H_4$)Ethylene glycol and deuterium oxide were obtained from Cambridge Isotope Laboratories, Inc. Sodium (2-$^{13}$C)pyruvate and (1-$^{13}$C)glycine were obtained from Icon Isotopes. (4*S*)-(4-$^2H_1$)NADPH was synthesized and purified using published procedures.[22,23] DXP was synthesized and purified as described previously.[24] $^1$H and $^{13}$C NMR spectra were acquired on a Varian INOVA 500 spectrometer equipped with a $^1$H,$^{13}$C,$^{15}$N probe using default pulse sequences.

***E. coli* DXR Expression and Purification.** BL21(DE3) *E. coli* cells previously transformed with a plasmid resulting from the insertion of the gene encoding *E. coli* DXR (*Ec*DXR) into pCA24N were obtained from the NationalBioResource Project, Japan (NBRP-*E. coli* at NIG).[25] Cultures were inoculated and grown at 37 °C to an $OD_{600}$ of 0.5−0.6 in LB-Miller broth containing 25 μg/L chloramphenicol. Optimal expression was achieved via induction with 500 μM IPTG at 31 °C for 4 h. Cell lysis and protein purification and storage were performed as described for *Mt*DXR.

**Synthesis of 2MGA.** (2*R*)-2,3-Dihydroxy-*N*-methoxy-2,*N*-dimethylpropionamide (**3**) was synthesized as reported previously[3] and reduced for 1 h in THF at 0 °C with 1.25 equiv of $LiAlH_4$. The resulting product was hydrolyzed in the presence of 1 M $NaHSO_4$ and desalted upon treatment with Amberlite IRA-400 ($OH^-$) and Amberlite IR-120 ($H^+$) ion-exchange resins to yield colorless oil (75% isolated yield). $^1$H NMR (500 MHz, $D_2O$): δ 9.61 (s, 1H, aldehyde), 4.92 (s, $^1$H, hydrate), 3.89 (d, *J* = 12.1 Hz, 1H, aldehyde), 3.63 (d, *J* = 12.1 Hz, 1H, aldehyde), 3.60 (d, *J* = 11.7 Hz, 1H, hydrate), 3.53 (d, *J* = 11.7 Hz, 1H, hydrate), 1.27 (s, 3H, aldehyde), 1.14 (s, 3H, hydrate). ESI-MS calcd for [2M+Na$^+$] $C_{18}H_{16}O_6Na$: 231.08, found 231.10. ee = 94%. As steady-state kinetic parameters of 2MGA turnover by *Mt*DXR were found to be stock-dependent, the synthetic route to 2MGA was altered to improve product purity. Details of the altered synthesis of 2MGA, enantiomeric excess determination, and quantification of the final stocks can be found in the Supporting Information.

**Synthesis of MEsP.** 2,3-*O*-Isopropylidene-2-*C*-methyl-D-erythrofuranose was synthesized from D-arabinose (**7**) as reported previously[1] and converted to dibenzyl 2,3-*O*-isopropylidene-2-*C*-methyl-D-erythrose 4-phosphate (**8**) according to the published procedure.[2] The resulting product was deprotected and quantified according to procedures described in the Supporting Information. The $^1$H NMR spectrum of the product was in agreement with that previously reported.[26]

**Synthesis of (2-$^{13}$C;3,4,4-$^2H_3$)DE.** (1,2,2-$^2H_3$)Glycolaldehyde was prepared enzymatically starting from (1,1,2,2-$^2H_4$)ethylene glycol as described for nonlabeled glycolaldehyde with certain modifications.[27] To a 1 M solution (final volume 1 mL) of (1,1,2,2-$^2H_4$)ethylene glycol in 0.8 M Tris-HCl, pH 9.0, and in $D_2O$ (87% v/v final) was added 100 U *P. pastoris* alcohol oxidase and 3000 U bovine liver catalase. The reaction mixture was stirred at 5 °C for 60 h resulting in 70% conversion to (1,2,2-$^2H_3$)glycolaldehyde-Tris imine. (2-$^{13}$C;3,4,4-$^2H_3$)DE was subsequently synthesized enzymatically by DXS-catalyzed condensation of (1,2,2-$^2H_3$)glycolaldehyde with sodium (2-$^{13}$C)pyruvate and purified as described previously for unlabeled DE.[16] $^1$H NMR (500 MHz, $D_2O$): δ 2.27 (d, *J* = 5.9 Hz, 3H).$^{13}$C NMR (125 MHz, $D_2O$): δ 215.4.

**Synthesis of (2-$^{13}$C)DE.** (2-$^{13}$C)DE was prepared as described above using unlabeled glycolaldehyde. $^1$H NMR (500 MHz, $D_2O$): δ 4.42 (dd, *J* = 7.3, 3.5 Hz, 1H), 3.95 (ddd, *J* = 12.3, 4.2, 1.5 Hz, 1H), 3.89 (ddd, *J* = 12.3, 5.0, 3.4 Hz, 1H), 2.27 (d, *J* = 5.9 Hz, 3H). $^{13}$C NMR (125 MHz, $D_2O$): δ 215.5.

**Steady-State Kinetics.** Measurement of initial velocities of DE and 2MGA turnover was performed using an Applied Photophysics SX-20 stopped flow spectrophotometer fit with a 20 μL flow cell (1 cm path length). The stopped-flow instrument was employed in preference to a conventional spectrophotometer primarily to reduce reactant quantities; unlike the reactions with the natural substrate DXP, no additional kinetic events were observed within the initial second of detection. Final assay mixtures with DE as a substrate contained 0−50 mM sodium phosphite buffer (pH 7.5), 25 mM Tris-HCl buffer (pH 7.5), 10 mM $MgCl_2$, 10 mM DTT, 200 μM NADPH, 1.5−40 mM DE, and 2.5 μM *Mt*DXR at an ionic strength of 0.2 M adjusted with NaCl. Final assay mixtures with 2MGA as a substrate contained 0−50 mM sodium phosphite buffer (pH 7.5), 25 mM HEPES buffer (pH 7.5), 10 mM $MgCl_2$, 200 μM NADPH, 1.5−35 mM 2MGA (aldehyde and hydrate form), and 2.5 μM *Mt*DXR at an ionic strength of 0.2 M adjusted with NaCl. 2MGA solutions were preincubated overnight at room temperature to minimize dimer formation. Measurement of initial velocities of MEsP and DXP turnover was performed using Varian Cary 3E UV−vis spectrophotometer. Final assay mixtures for measurement of inhibition of *Mt*DXR-catalyzed DXP turnover by phosphite dianion contained 0−50 mM sodium phosphite buffer (pH 7.5), 25 mM Tris-HCl buffer (pH 7.5), 10 mM $MgCl_2$, 10 mM DTT, 200 μM NADPH, 0.05−2


DOI: 10.1021/ja512911f
J. Am. Chem. Soc. 2015, 137, 2748−2756

**Table 1. Steady-State Kinetic Parameters and Kinetic Isotope Effects on the Hydride Transfer Step for DXP, MEsP, DE, and 2MGA Reactions Catalyzed by *Mt*DXR**

| | substrate | | | | | |
|---|---|---|---|---|---|---|
| kinetic parameter[a] | DXP[b] | MEsP | DE[c] | DE + $HPO_3^{2-}$[c] | 2MGA | 2MGA + $HPO_3^{2-}$ |
| $k_{cat}$ ($s^{-1}$) | 5.25 ± 0.19<br>18 ± 1[d] | 0.32 ± 0.04<br>9.8 ± 0.3[d] | (1.55 ± 0.12) × $10^{-3}$ | (8.6 ± 0.6) × $10^{-3}$ | (1.90 ± 0.40) × $10^{-3}$ | (4.42 ± 0.20) × $10^{-2}$ |
| $K_m$ (mM) | 0.115 ± 0.007<br>0.115 ± 0.014[d] | 0.040 ± 0.004<br>0.054 ± 0.005[d] | 53 ± 5 | 53 ± 5 | 6.6 ± 0.4 | 6.6 ± 0.4 |
| $K_{HPi}$ (mM) | N/A | N/A | N/A | 26 ± 4[e] | N/A | 13 ± 1[e] |
| $k_{cat}/K_m$ ($M^{-1}$ $s^{-1}$) | (4.6 ± 0.3) × $10^4$ | (8.1 ± 0.3) × $10^3$ | 0.0292 ± 0.0018 | 0.163 ± 0.010 | 0.29 ± 0.07 | 6.7 ± 0.2 |
| $^D(V/K)$ | 2.2 ± 0.2 | 1.0 ± 0.1 | N/A[f] | 1.1 ± 0.1 | 1.08 ± 0.06 | 1.09 ± 0.05 |
| $^DV$ | 1.35 ± 0.04 | 1.71 ± 0.04 | N/A[f] | 1.0 ± 0.2 | 1.11 ± 0.16 | 1.05 ± 0.06 |

[a]Errors are standard errors from global fitting. [b]From Liu and Murkin[21] except as noted. [c]From Kholodar and Murkin.[16] [d]Measured with *Ec*DXR at 37 °C. [e]Concentration of dianion form calculated at pH 7.5, p$K_a$ ($H_2PO_3^-$) = 6.31 (determined from the pH of a 50 mM solution of sodium salt at 25 °C and $I$ = 0.2 M (NaCl) at a 1:1 monoanion:dianion ratio). [f]Not calculated due to the high error associated with measurement of rates.

mM DXP, and 50 nM *Mt*DXR at an ionic strength of 0.2 M adjusted with NaCl. For *Mt*DXR, final assay mixtures with MEsP as a substrate contained 100 mM HEPES buffer (pH 7.5), 10 mM $MgCl_2$, 150 μM NADPH, 0−300 μM MEsP (aldehyde form), and 50 nM *Mt*DXR. For *Ec*DXR, final assay mixtures with DXP or MEsP as a substrate contained 50 mM triethanolamine-HCl (pH 7.7), 3 mM $MgCl_2$, 2 mM DTT, 150 μM NADPH, 0−300 μM DXP or MEsP (aldehyde form), and 10 nM *Ec*DXR. Monitoring of the NADPH absorbance decay at 340 nm ($\varepsilon_{340}$ = 6.22 $mM^{-1}$ $cm^{-1}$) was performed at 25 °C for *Mt*DXR and 37 °C for *Ec*DXR.

Steady state kinetics data were analyzed by analytical nonlinear regression using Pro-Data Viewer (Applied Photophysics), GraphPad Prism (GraphPad Software, La Jolla, CA), and SigmaPlot Version 12.5 (Systat Software, San Jose, CA), and standard errors associated with fitting are reported. Kinetic parameters presented in Table 1 were obtained by global fitting of eq 2 to the data.

**KIE Determinations.** NADPH primary deuterium KIEs were measured by the direct comparison method (i.e., determination of $V$ and $V/K$ for NADPH and NADPD separately) by global fitting of steady-state data to eq 1,

$$\frac{v_0}{[E]_t} = \frac{k_{cat}[S]}{K_m(1 + F_iE_{V/K}) + [S](1 + F_iE_V)} \quad (1)$$

where $E_{V/K}$ and $E_V$ are the isotope effects minus 1 on $V/K$ and $V$, respectively, and $F_i$ is the fraction of deuterium. The 2,3,3-$^2H_3$ KIE was measured by competitive reaction of (2-$^{13}$C)- and (2-$^{13}$C;3,4,4-$^2H_3$)DE monitored by $^{13}$C NMR, similar to literature methods.[28,29] Samples (700 μL) contained 200 μM *Mt*DXR, 5 mM (2-$^{13}$C)DE, 5 mM (2-$^{13}$C;3,4,4-$^2H_3$)DE, 25 mM Tris-HCl, pH 7.8, 10 mM $MgCl_2$, 50 mM sodium phosphite, pH 7.8, 0.2 mM NADPH, and 10% v/v $D_2O$. (1-$^{13}$C)Glycine (20 mM) was used as an internal standard for calculation of the fraction of conversion, $F_1$. D-Glucose (15 mM) and glucose dehydrogenase (2 U) were added to regenerate NADPH. Acquisition, processing, and data analysis are described in the Supporting Information.

## RESULTS

**Synthesis of Truncated and Complete Reaction Intermediates.** Previously, 2MGA was synthesized in racemic form to serve as a potential alternative substrate of fructose-1,6-diphosphate aldolase.[30] To avoid ambiguity in interpretation of the kinetics with *Mt*DXR, we developed an enantioselective synthetic scheme (Scheme 2) leading predominantly to the D-isomer. This approach features asymmetric dihydroxylation of Weinreb amide **2**,[3] which was previously reported to proceed with 96.5% ee.[4] Reduction of the Weinreb amide by $LiAlH_4$ followed by hydrolysis with mild acid produced 2MGA with 94% ee. Attempts to purify 2MGA by flash chromatography were hampered by its instability in the presence of silica, which

**Scheme 2. Synthesis of 2-*C*-Methyl-D-glyceraldehyde (2MGA)[a]**

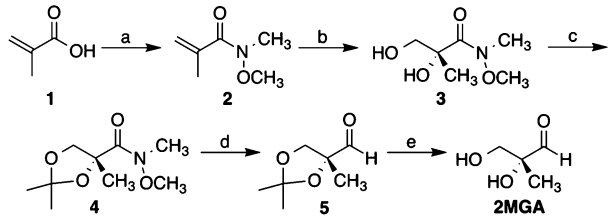


[a]Reaction conditions: (a) (i) $SOCl_2$, $CH_2Cl_2$; (ii) $CH_3ONHCH_3$·HCl, pyridine;[3] (b) modified α-AD mix;[4,5] (c) $Me_2C(OMe)_2$, *p*-$MeC_6H_4SO_3H$;[9] (d) $LiAlH_4$, THF; (e) Amberlite ($H^+$ form), $H_2O$.

was found to catalyze its quantitative rearrangement to DE (or its enantiomer). To facilitate purification, chiral Weinreb amide precursor **3** was converted to the acetonide,[9] reduced by $LiAlH_4$ to the corresponding aldehyde, and distilled under vacuum. Pure 2MGA was obtained following cleavage of the acetonide in the presence of Amberlite ($H^+$ form). To assess the effect of truncation on kinetics and KIEs for the reaction intermediate, we synthesized MEsP (Scheme 1, R = $CH_2OPO_3^{2-}$), initially following the procedure reported by Hoeffler and co-workers;[26] however, because of the formation of significant impurities, an alternative synthetic sequence was adapted from protocols for the synthesis of MEsP precursor dibenzyl 2,3-*O*-isopropylidene-2-*C*-methyl-D-erythrose 4-phosphate (**8**) (Scheme 3).[1,2]

**Steady-State Kinetics.** The kinetics of MEsP reduction by *Mt*DXR was measured in the presence of saturating concentrations of NADPH and $Mg^{2+}$ and varying MEsP (0−200 μM final, as aldehyde) (Table 1). To permit comparison with literature,[26] steady-state kinetic parameters were also measured for *Ec*DXR in the previously reported conditions.

**Scheme 3. Synthesis of 2-*C*-Methyl-D-erythrose 4-Phosphate (MEsP)[a]**

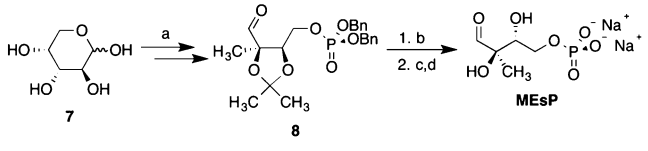


[a]Reaction conditions: (a) From refs 1, 2; (b) $H_2$, Pd/C, MeOH; (c) 37 °C, $H_2O$ (9 h); (d) 1 M NaOH.



DOI: 10.1021/ja512911f
J. Am. Chem. Soc. 2015, 137, 2748−2756

While our value of $k_{cat}$ = 9.8 ± 0.3 $s^{-1}$ agrees favorably with the reported value of ~8 $s^{-1}$ (calculated from specific activity), the $K_m$ value of 54 ± 5 μM (aldehyde form) was found to be three times less than the reported value of 158 μM.[26] Since the concentration of MEsP in the previous study was determined enzymatically, the reported value of $K_m$ likely reflects the total concentration of MEsP (aldehyde and hydrate forms). Consequently, the $K_m$ value could have been overestimated by the factor of $(1 + K_{hyd})$, where $K_{hyd}$ = 1.0 at 37 °C.

In this work we have assumed that isomerization of the truncated substrate DE results in formation of the truncated intermediate 2MGA, which undergoes reduction to the final product 2MG (Scheme 1, R = H).[16] Similar to observations with the complete intermediate, incubation of 2MGA and NADPH with *Mt*DXR in the presence of phosphite dianion was found to produce 2MG. Interestingly, when 2MGA was incubated with $NADP^+$ and *Mt*DXR in the presence of phosphite dianion, only 2% of the starting material was converted to DE; the remaining 98% of 2MGA was observed to disproportionate to 2MG and 2-*C*-methyl-D-glyceric acid (Figure S1). When monitored spectrophotometrically, transient formation of NADPH was observed upon incubation of 2MGA with $NADP^+$ and *Mt*DXR (Figure S2), suggesting direct oxidation of the hydrate form of 2MGA to 2-*C*-methyl-D-glyceric acid, followed by reduction of the aldehyde form of 2MGA by the generated NADPH. In contrast, the complete intermediate MEsP was found to predominantly partition toward DXP in the presence of $NADP^+$ and *Mt*DXR, with only 24% undergoing disproportionation (Figure S3).

To investigate the effect of truncation on the kinetic parameters of intermediate turnover, the kinetics of *Mt*DXR-catalyzed reduction of 2MGA was assayed by monitoring NADPH absorbance upon mixing a 1:1 volume ratio of solutions containing enzyme (2.5 μM final) and varying 2MGA (0–5.9 mM final, as aldehyde), respectively. Both solutions also contained saturating NADPH (200 μM) and varying phosphite dianion (0–50 mM), and a constant ionic strength of 0.2 M was maintained by addition of NaCl. As reported in our previous work, due to the much lower $K_m$ of NADPH (9.8 μM), an ordered sequential mechanism with NADPH preceding 2MGA was assumed.[20,21] The data revealed hyperbolic dependences on both ligands (Figure 1), consistent with non-essential activation by phosphite (Scheme 4).[31] In this scheme, $k_{cat}$ and $k'_{cat}$ are the respective first-order rate constants in the absence and presence of phosphite, $k_1$, $k_{-1}$, $k_2$, and $k_{-2}$ are the rate constants for 2MGA binding to form its ternary (*Mt*DXR·NADPH·2MGA) and quaternary (*Mt*DXR·NADPH·2MGA·$HPO_3^{2-}$) complexes, and $K_3$ and $K_4$ are the respective dissociation constants for phosphite from its ternary and quaternary complexes. Equation 2 describes the kinetics of activation under assumption of either (1) rapid equilibrium ligand binding and independence of dissociation constants on the presence of the other ligand (i.e., $k_{-1}/k_1 = k_{-2}/k_2 = K_m$ and $K_3 = K_4 = K_{HPi}$), or (2) rapid equilibrium binding of phosphite where $K_{HPi} = K_4$ and steady-state binding of 2MGA under conditions that provide a constant $K_m$ (i.e., $(k_{cat} + k_{-1})/k_1 = (k'_{cat} + k_{-2})/k_2$; refer to the Discussion for details). The first- and second-order rate constants as well as $K_m$ and $K_{HPi}$ (Table 1) were obtained by global fitting of the rate equation (eq 2)[31] to the data.

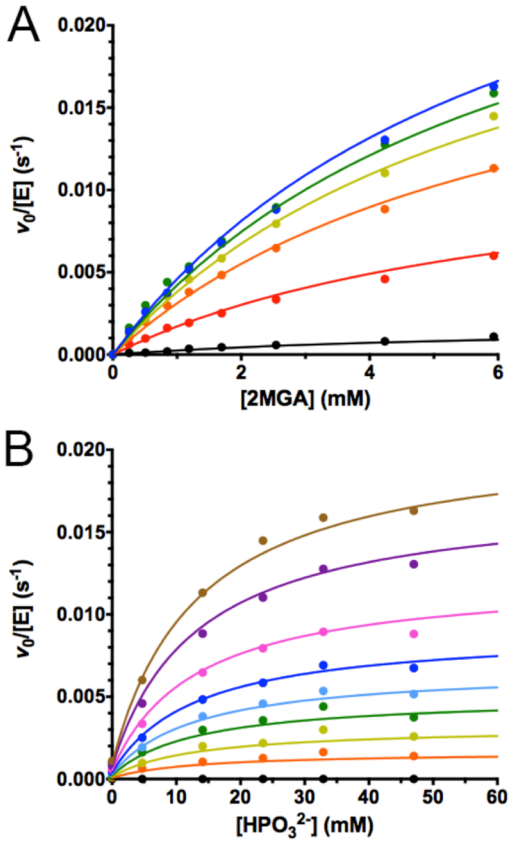


**Figure 1.** Dependence of the rate of *Mt*DXR-catalyzed 2MGA turnover on the concentrations of (A) 2MGA ([$HPO_3^{2-}$], from bottom to top: 0, 4.7, 14.1, 23.5, 32.9, and 47.0 mM) and (B) phosphite dianion ([2MGA], from bottom to top: 0, 0.5, 0.8, 1.2, 1.7, 2.5, 4.2, and 5.9 mM) at pH 7.5, 25 °C ($I$ = 0.2 M, NaCl). Curves are the result of nonlinear regression performed globally using eq 2.

**Scheme 4. Non-essential Activation Model for Phosphite-Activated 2MGA Turnover by *Mt*DXR[a]**

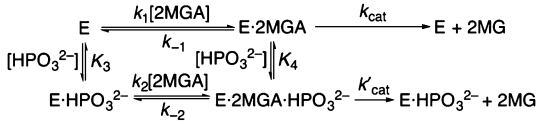


[a] E = *Mt*DXR·NADPH.

$$\frac{v_0}{[E]_t} = \frac{(k_{cat}K_{HPi} + k'_{cat}[HPO_3^{2-}])[2MGA]}{[2MGA][HPO_3^{2-}] + K_m[HPO_3^{2-}] + K_{HPi}[2MGA] + K_mK_{HPi}} \quad (2)$$

**Kinetic Isotope Effects.** To study the effect of covalently linked phosphodianion on the contribution of hydride transfer step to the reaction coordinate, primary deuterium KIEs originating from deuterium substitution at the C-4 pro-*S* position of the dihydronicotinamide ring of NADPH were measured. KIEs on parameters $k_{cat}$, symbolized $^DV$, and $k_{cat}/K_m$, symbolized $^D(V/K)$, were measured using a direct comparison method for the reactions of substrate and intermediate in pieces (Figure S5) and compared with the corresponding KIEs determined for the reactions of DXP (reported in literature) and MEsP (this work, Figure S4) (Table 1).


DOI: 10.1021/ja512911f
J. Am. Chem. Soc. 2015, 137, 2748–2756

To test whether the carbon-skeleton rearrangement is a significant contributor to the reaction coordinate for the substrate in pieces, a deuterium KIE on this step was determined using trideuterated DE. Labeling of the three hydrogen atoms at C-3 and C-4 was chosen based on the ease of synthesis and the expected increased magnitude of the resultant KIE, due to the multiplicative effect of the three $sp^3 \rightarrow sp^2$ hybridization changes associated with retro-aldolization. Labeling was accomplished by a chemoenzymatic synthesis (Scheme S1). Commercial ($^2H_4$)ethylene glycol was selectively oxidized by *P. pastoris* alcohol oxidase to form (1,2,2-$^2H_3$)-glycolaldehyde, as reported in literature.[27] In order to prevent $\alpha$-deuterium washout from the product,[12] the reaction was conducted in 87% $D_2O$. Double oxidation to glyoxal was circumvented by the inclusion of Tris base, which readily forms an imine with glycoladehyde as it is released from the oxidase. This reversible adduct was competent in subsequent decarboxylative condensation with (2-$^{13}$C)pyruvate catalyzed by DXS. (2-$^{13}$C)- and (2-$^{13}$C;3,4,4-$^2H_3$)DE were prepared by this route using unlabeled and deuterated ethylene glycol, respectively, and purified by flash column silica gel chromatography as described previously.[16] An internal competition experiment based on the $^{13}$C NMR technique of Bennet and co-workers[28] was employed to measure the KIE. In this procedure, the $^{13}$C signal at C-2 serves as a reporter for the neighboring isotope substitution, appearing as resolved singlets for (2-$^{13}$C)DE and (2-$^{13}$C;3,4,4-$^2H_3$)DE whose chemical shifts differ by ∼0.1 ppm due to an isotope effect on the nuclear shielding.[32] The ratio of heavy to light isotopologue ($R$) was calculated by integration and plotted as a function of the fraction of conversion of light isotopologue ($F_1$) (Figure S6), to which eq 3 was fit to yield a KIE of 1.25 ± 0.02.[29]

$$R = R_0(1 - F_1)^{(1/\mathrm{KIE}-1)} \quad (3)$$

**Determination of the Structure of *Mt*DXR with the Substrate in Pieces.** The structure of *Mt*DXR bound to NADPH, $Mn^{2+}$, $HPO_3^{2-}$, and DE was solved at 2.3 Å resolution. The electron density revealed differences between the two chains in the asymmetric unit and will be described separately. The electron density for Chain B is of poorer overall quality. The chain contains Gly11-Met389 in the final model. Density for the active site loop is of modest quality; however, all but His200 and Pro201 are present in the final model. While density for the metal ion was clear, no density is present for the truncated substrate. Additionally, the density for the nucleotide cofactor showed partial occupancy. The NADPH molecule was not present at full occupancy and was built containing the only 2′-phosphoribose and the diphosphate linker between the two nucleotides.

The final model for chain A contains residues Arg12-Met389 has better density and shows clear density for all three ligands (Figure S8). This chain was used for all analysis. The active site loop, Ala189 through Gly206, is disordered and not included in the final density. There is weak density for Ser204 and Met205 from this loop however it was not of sufficient quality to be included in the final model. The active site of chain A shows clear density for the $Mn^{2+}$ ion, NADPH, a molecule of DE, and one $HPO_3^{2-}$ ion. Unlike the natural substrate, the DE ligand coordinates the metal ion in a tridentate fashion. Cleavage of the linkage between the phosphate/phosphite and the remainder of the molecule allows the deoxy sugar to form a more compact orientation that donates three oxygens to the $Mn^{2+}$ ion.

## DISCUSSION

**Chemical Competence of Intermediates.** The aldehyde intermediate of the DXR-catalyzed interconversion between DXP and MEP, MEsP (Scheme 1, R = $CH_2OPO_3^{2-}$), was proposed in early studies of the MEP pathway[33] but its generation has never been directly observed.[19,26,34] Our studies revealed that synthetic MEsP is converted to MEP by *Ec*DXR and *Mt*DXR in the presence of NADPH, confirming MEsP's chemical competence reported previously.[26] Likewise, 2MGA was exclusively converted to 2MG in the presence of the reduced coenzyme. When the oxidized coenzyme was used, however, both intermediates were observed to undergo varying degrees of disproportionation in addition to the expected rearrangement to their respective ketone isomers. This aldehyde dehydrogenase activity by DXR had not been reported previously. The extent of disproportionation is considerably suppressed with MEsP, suggesting that its covalently linked phosphate group plays a role in the enzyme's ability to discriminate between aldehyde and hydrate forms of the intermediate.

**Kinetic Competence of Intermediates.** A candidate intermediate is considered kinetically competent when it reacts at a rate equal to or exceeding that of the substrate through the complete reaction pathway. The complete intermediate MEsP was previously demonstrated to be kinetically competent with *Ec*DXR, being turned over as fast as the substrate DXP.[26] Although we have independently reproduced the reported $k_{cat}$ (reported as specific activity) for turnover of MEsP by *Ec*DXR, the $k_{cat}$ for DXP under the same conditions was found to be 2-fold larger in our hands. An even larger difference was observed with *Mt*DXR, in which case MEsP exhibited a 16-fold lower first-order rate constant than that for DXP. Do these new results imply that MEsP is not an intermediate in the natural DXR reaction?

The observation of kinetic competence supports a compound's designated role as a reaction intermediate. A lack of kinetic competence, however, does not necessary imply that the compound cannot be a reaction intermediate. As noted by Cleland,[35] an exogenously added intermediate must first bind to the enzyme, a step that is absent when the intermediate is generated transiently in the active site. To be productive catalysts, most enzymes do not readily permit dissociation of their intermediates. Because excessively tight binding of the intermediate, defined by the ratio of dissociation and association rate constants, would preclude efficient turnover, it is not unusual for the slow dissociation to be accompanied by comparably slow association. Additionally, once bound, the intermediate might not adopt the same orientation as when produced transiently during the natural reaction. Hence, only if the rates of association and reorientation significantly exceed the substrate's $k_{cat}$ will an intermediate appear kinetically competent.

First, consider that MEsP binds to the E·NADPH complex to form a ternary complex E*·NADPH·MEsP (Scheme 5, lower pathway) distinct from that formed transiently during turnover of DXP (i.e., E·NADPH·MEsP; Scheme 5, upper pathway). Two possibilities can be envisioned from this point: (1) hydride transfer occurs with a rate constant $k_{10}$ much lower than $k_7$, or (2) a slow conformational change converts E*·NADPH·MEsP to E·NADPH·MEsP, which then undergoes hydride transfer.


DOI: 10.1021/ja512911f
J. Am. Chem. Soc. 2015, 137, 2748−2756

**Scheme 5. Simplified Kinetic Model for Turnover of DXP and MEsP**[a]

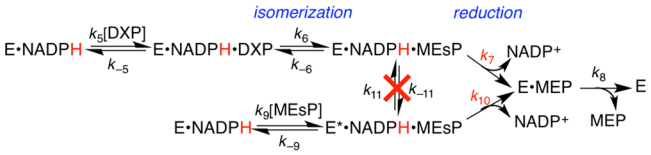


[a]The isotope (H or D) and isotope-sensitive step are in red.

The magnitude of the primary deuterium KIE on $k_{cat}$ for reduction of MEsP can distinguish between these possibilities.

KIEs for DXP turnover using (4*S*)-(4-$^2$H)NADPH (NADPD) were previously measured by the direct comparison method.[20,24,36] This method provides KIEs on both $k_{cat}/K_m$ and $k_{cat}$, given by eqs 4 and 5, which reflect different portions of the kinetic mechanism.

$$^{D}(V/K) = \frac{^{D}k + C_f + C_r\,^{D}K_{eq}}{1 + C_f + C_r} \quad (4)$$

$$^{D}V = \frac{^{D}k + C_{vf} + C_r\,^{D}K_{eq}}{1 + C_{vf} + C_r} \quad (5)$$

The intrinsic KIE, $^{D}k$, that would be observed if the isotope-sensitive step were completely rate-limiting is mitigated by the forward ($c_f$ for $^{D}(V/K)$ and $c_{vf}$ for $^{D}V$) and reverse ($c_r$) commitment factors and the equilibrium isotope effect for the overall reaction ($^{D}K_{eq}$). With DXP as the varied substrate, $^{D}(V/K)$ and $^{D}V$ were found to be 2.2 and 1.3, respectively (Table 1), indicating that reduction is partially rate limiting. Suppression of $^{D}V$ relative to $^{D}(V/K)$ is reflective of a larger $c_{vf}$. According to Scheme 5, the expressions for $c_f$ and $c_{vf}$ are described by eqs 6 and 7.[24]

$$c_f = \frac{k_7}{k_{-6}}\left(1 + \frac{k_6}{k_{-5}}\right) \approx \frac{k_7}{k_{-6}} \quad (6)$$

$$c_{vf} = \left(\frac{k_6k_7}{k_6 + k_{-6}}\right)\left(\frac{1}{k_6} + \frac{1}{k_8}\right) \quad (7)$$

The increased value of $c_{vf}$ and associated suppression of $^{D}V$ have been attributed to the slow release of the second product, MEP, under control of $k_8$.[21,24]

If exogenously added MEsP proceeds through direct, slow hydride transfer (case 1 above), $c_{vf}$ is given by eq 8; case 2 (slow conformational change) would provide $c_{vf}$ according to eq 9.

$$c_{vf} = \frac{k_{10}}{k_8} \quad (8)$$

$$c_{vf} = \left(\frac{k_7k_{11}}{k_{11} + k_{-11}}\right)\left(\frac{1}{k_{11}} + \frac{1}{k_8}\right) \quad (9)$$

These two cases differ in that the slow step for case 1, $k_{10}$, appears in the numerator, while that for case 2, $k_{11}$, appears in the denominator. The consequence of this is that eq 8 predicts a larger $^{D}V$ than that observed for DXP while eq 9 predicts a smaller $^{D}V$. The larger measured value of 1.7 (Table 1) is clearly inconsistent with case 2. Thus, we conclude that exogenous MEsP lacks kinetic competence because it binds and reacts in a conformation that is distinct from that adopted during turnover of DXP.

**Rate-Limiting Steps for Substrates and Intermediates.** KIEs are invaluable tools in establishing the mechanism of enzyme-catalyzed reactions, as exemplified in the preceding experiments with MEsP. The magnitudes of observed KIEs not only reveal the degree of rate limitation by the isotope-sensitive step, but also provide insights on the contribution of other steps, chemical or physical, to the reaction coordinate.

Primary deuterium KIEs[20] together with $^{13}$C KIEs for C-2, C-3, and C-4 of DXP previously measured with *Mt*DXR[29] indicate that isomerization and reduction are jointly rate-limiting processes with respect to $k_{cat}/K_m$ for DXP. With removal of the rearrangement step and in light of the $^{D}V$ = 1.7, one might expect $^{D}(V/K)$ for MEsP to surpass the value of 2.2 measured for DXP (Table 1); interestingly, this was found to be unity, indicating that hydride transfer is completely masked by the forward commitment factor. According to Scheme 5, $c_f$ is given by eq 10.

$$c_f = \frac{k_{10}}{k_{-9}} \quad (10)$$

The absence of a KIE on $k_{cat}/K_m$ suggests that MEsP is a "sticky" substrate in which it preferentially partitions from the Michaelis complex through the chemical reaction rather than dissociating (i.e., $k_{-9} < k_{10}$). Given that dissociation of the *transiently formed* intermediate has never been observed during DXP turnover, it can be expected to be similarly sticky.

A similar KIE analysis was performed with the truncated substrate and intermediate in order to explore the energetic consequences of severing the phosphodianion's covalent linkage and of its removal from the reaction. Unlike the reactions of DXP and MEsP, the reactions of the substrate and intermediate in pieces were found to exhibit KIEs of unity on both $k_{cat}$ and $k_{cat}/K_m$. To test if the absence of KIEs in the reaction of the substrate in pieces is the result of fully rate-limiting isomerization, a combined $\alpha$-secondary 3,4,4-$^2H_3$ KIE was measured for DE. The observed value of 1.25 represents an average of 1.08 per $^2$H, which is smaller than the typical values of 1.15−1.35[37,38] for such sp$^3$ → sp$^2$ rehybridization. Thus, although the isomerization step is rate contributing in DE turnover, a non-chemical step such as a conformational change likely also contributes to rate limitation. In the case of the intermediate in pieces, the absence of KIEs during reduction also implicates a rate-limiting physical step. Since both $^{D}V$ and $^{D}(V/K)$ are suppressed, this step must occur after formation of the Michaelis complex with 2MGA and before the first irreversible step (presumably release of the first product). Thus, a mechanism consistent with the above KIE experiments is identical to Scheme 5 but with an additional ternary complex between isomerization and reduction steps (Scheme S2).

**Kinetic Role of the Phosphodianion Group.** In our previous study we demonstrated that removal of the terminal phosphorylmethyl group of DXP results in a $10^6$-fold decrease in turnover rate.[39] Therefore, according to the Eyring equation (eq S2), the nonreacting phosphodianion group provides $\Delta G_{Pi}$ = 8.4 ± 0.1 kcal/mol of the average kinetic barrier stabilization. Interestingly, the same analysis applied to the reaction of the intermediate revealed a substantially lower $\Delta G_{Pi}$ of 6.1 ± 0.1 kcal/mol. Although this result may appear to indicate that the phosphodianion provides more stabilization during isomerization than reduction, the factor(s) responsible for the apparent "kinetic incompetence" of MEsP likely suppresses the actual stabilization energy.



DOI: 10.1021/ja512911f
J. Am. Chem. Soc. 2015, 137, 2748−2756

The kinetic barrier destabilization resulting from substrate and intermediate truncation was partially relieved by inorganic phosphite dianion. While the reaction of truncated substrate experienced only 5-fold activation by saturating phosphite, the reaction of exogenous truncated intermediate was activated by a factor of 23. Importantly, in each case an equivalent increase in both the first-and second-order rate constants was observed, indicating that the observed activation is the result of a catalytic effect rather than a binding effect. Accordingly, interactions of the active site with phosphite dianion provided $\Delta G_{HPi} = 3.2 \pm 0.1$ kcal/mol and $\Delta G_{HPi} = 4.4 \pm 0.2$ kcal/mol of kinetic barrier stabilization for turnover of DE and 2MGA, respectively (eq S3). Since DE turnover is partially limited by chemistry and 2MGA turnover is entirely limited by physical steps, the greater phosphite binding energy observed during 2MGA turnover suggests an increased role of phosphodianion−enzyme interactions in acceleration of the physical steps.

The increase in the activation factor observed for 2MGA turnover was also accompanied by a 2-fold decrease in $K_{HPi}$, the concentration of phosphite dianion required to reach half-maximal activation. Recall that the data for each substrate treated separately is consistent with a random binding mechanism (Scheme 4). The independence of $K_{HPi}$ with respect to 2MGA concentration (Figure 1B) suggests that the affinities of phosphite dianion to E·NADPH and E·NADPH·2MGA are equal. Because the non-essential activation models for both substrates share a common binding of phosphite dianion to E·NADPH ($K_3$ in Scheme 4), the observed $K_{HPi}$ should be identical for DE and 2MGA under equilibrium binding conditions. To evaluate this apparent discrepancy, we independently determined $K_3$ by measuring a $K_i = 28 \pm 4$ mM for competitive inhibition by phosphite dianion with respect to DXP. This $K_i$ favorably agrees with the $K_{HPi} = 26$ mM determined with DE as substrate,[16] thus validating the rapid-equilibrium random non-essential activation model previously invoked with this substrate; the lower value of $K_{HPi}$ in the case of 2MGA turnover therefore suggests a change in the kinetic mechanism with the truncated intermediate. To account for this change we have assumed rapid equilibrium binding of phosphite and steady-state binding of 2MGA, and we have required phosphite binding to be 2-fold tighter to E·NADPH·2MGA than to E·NADPH (i.e., $K_3 = 2K_4$). The thermodynamic box therefore also requires $k_{-1}/k_1 = 2k_{-2}/k_2$. Further, in order to maintain a $K_m$ independent of phosphite concentration, this scheme requires satisfaction of eq 11.

$$K_m = \frac{k_{cat} + k_{-1}}{k_1} = \frac{k'_{cat} + k_{-2}}{k_2} \tag{11}$$

If $k_1 = k_2$, then $k_{-1} = 2k_{-2}$, allowing an estimation of $k_{-1} = 0.084$ $s^{-1}$ and $k_{-2} = 0.042$ $s^{-1}$ using the values of $k_{cat}$ and $k'_{cat}$ from Table 1. The rate equation for such a kinetic model is identical to eq 2 (see derivation in Supporting Information). From this analysis we conclude that the rate of 2MGA release from the enzyme must be of similar magnitude to its turnover. However, such a scenario would predict release and detectable accumulation of 2MGA during transient turnover of DE. Because we have never observed such accumulation in the absence or presence of phosphite dianion, the kinetic pathways involving exogenous and transient 2MGA are likely distinct, not unlike the situation with MEsP. Nevertheless, the reaction of exogenous 2MGA is a useful model system, revealing tightening of the interactions between the enzyme and phosphodianion when the active site is occupied by the intermediate. Additionally, this model suggests slower release of the truncated intermediate from the phosphite dianion-bound active site. One may reasonably propose similar effects to take place during the formation of transient 2MGA. Interestingly, according to the thermodynamic box in Scheme 6, tightening of phosphite−enzyme interactions at the intermediate stage of the reaction (i.e., $K_{15} < K_{14}$) would require a proportional increase in the equilibrium constant for the conversion of the substrate to the intermediate (i.e., $K_{13} = K_{12}\,K_{14}/\,K_{15}$).

**Scheme 6. Thermodynamic Box Describing Conversion of DE to 2MGA in the Absence and Presence of Phosphite Dianion**[a]

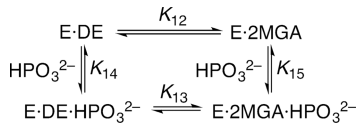


[a]E = *Mt*DXR·NADPH.

**Structural Rationale for the Role of the Phosphodianion.** To directly assess the nature of physical steps implicated in rate limitation of the reaction of the substrate in pieces, we co-crystallized *Mt*DXR with the complete set of ligands involved in this reaction. The structure resolved in this work is the first example of DXR crystallized as a catalytically active complex containing a substrate, NADPH, and divalent metal. Contrary to our previous hypothesis that phosphite dianion bound in the active site stabilizes the closed conformation of the enzyme,[16] we did not observe electron density for the flexible catalytic loop 189−206 in the enzyme subunit bound to DE, NADPH, and $HPO_3^{2-}$. The absence of electron density suggests disorder in the loop, thus supporting our proposal that the covalent linkage to the phosphodianion is required to assist induction of productive enzyme conformations. With the exception of this loop, the overall enzyme conformation is conserved in structures of *Mt*DXR bound with the substrate in pieces and with inhibitor FR-900098[40] (Figure S8). The active-site cleft located between N- and C-terminal domains is visibly more closed in the structure with inhibitor, thus making it a more-compact and tight complex.

The orientation of the truncated substrate likely reflects a non-productive binding mode, as the molecule is positioned with the C-1 methyl group proximal to the dianion (Figure 2), unlike FR-900098 and DXP. The retro-aldol step requires deprotonation of the alcohol at C-4 to generate glycolaldehyde phosphate (from DXP) or formaldehyde (from DE) (Scheme 1). Although the enzymatic base has not yet been identified, it is likely positioned proximal to C-4, which occupies the same space as the C-1 methyl group of DE in the crystal structure; thus, reorientation of DE would be expected for reaction to take place, an action that likely requires dissociation, rotation, and re-association. Further, all three oxygen atoms in DE coordinate the catalytic divalent metal. The C-4 hydroxyl group may need to sever its coordinate bond in order to assume a conformation poised for proton transfer to the catalytic base. The covalently linked phosphodianion of DXP restricts rotation along the carbon backbone making tridentate coordination highly unlikely for the complete substrate, assuming its binding mode resembles that of FR-900098; thus, the attached


DOI: 10.1021/ja512911f
J. Am. Chem. Soc. 2015, 137, 2748−2756

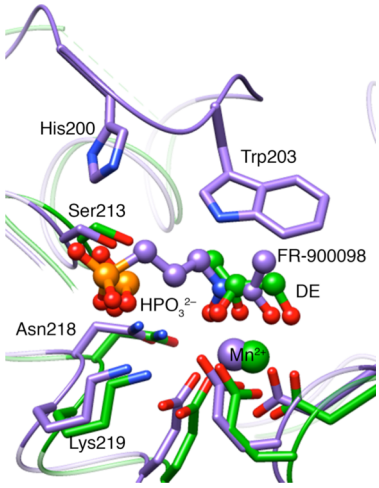


**Figure 2.** Superposition of the crystal structures of *Mt*DXR with inhibitor FR-900098, $Mn^{2+}$, and NADPH (not shown) (PDB entry 4A03, purple) and *Mt*DXR with DE, $Mn^{2+}$, NADPH (not shown), and $HPO_3^{2-}$ (PDB entry 4RCV, green). Residues of the flexible loop, phosphodianion binding pocket, and metal-binding pocket are shown. Loop 189−206 is absent in the structure with the substrate in pieces (green).

phosphoryl group may facilitate adoption of a reactive conformation in DXP.

The position of phosphite in the phosphate-binding pocket partially overlaps the position of the phosphonate group of FR-900098 (Figure 2). Both groups are in the proximity to establish hydrogen bonds with Lys219, Asn218, and Ser213. A hydrogen bond (or salt bridge) with His200 is considered crucial for the closure of the flexible loop upon binding of the phosphodianion of the ligand.[41] It is possible that a similar interaction exists with phosphite dianion.

## CONCLUSION

The deconstruction of ligands in order to determine binding modes and activities of the resulting fragments lies at the core of fragment-based drug design, an approach rapidly eclipsing classical structure-based drug design.[42] However, a recent systematic study demonstrated that application of the same approach to substrate discovery is particularly challenging and system dependent.[43] The work in this manuscript addresses the energetic and structural effects of removal of the covalent linkage to the phosphoryl group in the substrate and intermediate of a multistep enzymatic reaction.

In summary, we have demonstrated the following functional relationships between the nonreacting phosphodianion and catalysis at different stages of the reaction. (1) The absence of the covalent linkage to the phosphate compromises the enzyme's specificity for the true (aldehyde) form of the reaction intermediate. A promiscuous conformation of *Mt*DXR induced by separate phosphodianion exhibits a novel aldehyde dehydrogenase activity. (2) Highly orchestrated progress of the reaction does not allow the release of transiently formed intermediate in the absence or presence of the covalently linked phosphodianion. This assertion is reinforced by the apparent inability of the enzyme to adopt the transiently formed conformation during turnover of the exogenous intermediates. (3) While the rate of the reaction of the phosphorylated substrate is limited by both chemical steps, reaction of the substrate in pieces is predominantly limited by physical steps, displaying only partial rate limitation from isomerization. (4) The loss of interactions with the covalently linked phosphate result in 8.4 and 6.1 kcal/mol destabilization of the kinetic barriers to turnover of substrate and exogenous intermediate, respectively. Part of this energy (3.2 and 4.4 kcal/mol, respectively) is recovered by inclusion of phosphite dianion, which thereby serves as a non-essential activator of both reaction steps. (5) At the intermediate stage of the reaction, there is a tightening of the interactions between the active site and the phosphodianion, which results in a corresponding increase in the equilibrium between substrate and intermediate. (6) The structure of the *Mt*DXR complex with the substrate in pieces underscores the role of the covalently linked phosphate in promoting the productive orientation of the substrate and induction of the loop-closed conformation associated with efficient catalysis.

## ASSOCIATED CONTENT

### Supporting Information

2MGA and MEsP synthesis; $^1$H NMR spectra of reactions with 2MGA, DE, and MEsP; $A_{340}$ transient for time course of the incubation of 2MGA with $NADP^+$ and *Mt*DXR; Michaelis−Menten plots for primary deuterium KIEs; determination of the (3,4,4-$^2H_3$)DE KIE; crystallographic details and refinement statistics; electron density for ligands of *Mt*DXR in its crystal structure with substrate in pieces, comparison of conformations of FR-900098-bound and substrate in pieces-bound *Mt*DXR subunits. This material is available free of charge via the Internet at http://pubs.acs.org.

## AUTHOR INFORMATION

### Corresponding Author

*amurkin@buffalo.edu

### Notes

The authors declare no competing financial interest.

## ACKNOWLEDGMENTS

This work was supported by a DuPont Young Professor Grant and NSF CAREER Award CHE1255136 (to A.S.M.) and NIH Grant GM-068440 (to A.M.G.). We thank Jeffrey Marvin and Margaret Moynihan for expression and purification of *Ec*DXR, and Dr. Gregory Tombline for preparation of DXP.

## REFERENCES

(1) Koumbis, A. E.; Kaitaidis, A. D.; Kotoulas, S. S. *Tetrahedron Lett.* **2006**, *47*, 8479.
(2) Kis, K.; Wungsintaweekul, J.; Eisenreich, W.; Zenk, M. H.; Bacher, A. *J. Org. Chem.* **2000**, *65*, 587.
(3) Smith, N. D.; Goodman, M. *Org. Lett.* **2003**, *5*, 1035.
(4) Avenoza, A.; Cativiela, C.; Corzana, F.; Peregrina, J. M.; Sucunza, D.; Zurbano, M. M. *Tetrahedron: Asymmetry* **2001**, *12*, 949.
(5) Bennani, Y. L.; Sharpless, K. B. *Tetrahedron Lett.* **1993**, *34*, 2079.
(6) Amyes, T. L.; Richard, J. P. *Biochemistry* **2007**, *46*, 5841.
(7) Amyes, T. L.; O'Donoghue, A. C.; Richard, J. P. *J. Am. Chem. Soc.* **2001**, *123*, 11325.
(8) Richard, J. P. *Biochemistry* **2012**, *51*, 2652.
(9) Aicher, T. D.; Boyd, S. A.; Chicarelli, M. J.; Condroski, K. R.; Fell, J. B.; Fischer, J. P.; Gunawardana, I. W.; Hinklin, R. J.; Singh, A.; Turner, T. M.; Wallace, E. M. Preparation of Pyridin-2-Ylamino-1,2,4-Thiadiazole Derivatives as Glucokinase Activators for the Treatment of Diabetes Mellitus. Patent WO 2009042435, April 2, 2009.
(10) Amyes, T. L.; Richard, J. P.; Tait, J. J. *J. Am. Chem. Soc.* **2005**, *127*, 15708.


DOI: 10.1021/ja512911f
*J. Am. Chem. Soc.* 2015, 137, 2748−2756

(11) Tsang, W. Y.; Amyes, T. L.; Richard, J. P. *Biochemistry* **2008**, *47*, 4575.
(12) Amyes, T. L.; Richard, J. P. *Biochemistry* **2013**, *52*, 2021.
(13) Malabanan, M. M.; Amyes, T. L.; Richard, J. P. *Curr. Opin Struct Biol.* **2010**, *20*, 702.
(14) Morrow, J. R.; Amyes, T. L.; Richard, J. P. *Acc. Chem. Res.* **2008**, *41*, 539.
(15) Jencks, W. P. *Adv. Enzymol. Relat. Areas Mol. Biol.* **1975**, *43*, 219.
(16) Kholodar, S. A.; Murkin, A. S. *Biochemistry* **2013**, *52*, 2302.
(17) Murkin, A. S.; Manning, K. A.; Kholodar, S. A. *Bioorg. Chem.* **2014**, *57*, 171.
(18) Perruchon, J.; Ortmann, R.; Altenkamper, M.; Silber, K.; Wiesner, J.; Jomaa, H.; Klebe, G.; Schlitzer, M. *ChemMedChem.* **2008**, *3*, 1232.
(19) Takahashi, S.; Kuzuyama, T.; Watanabe, H.; Seto, H. *Proc. Natl. Acad. Sci. U.S.A.* **1998**, *95*, 9879.
(20) Argyrou, A.; Blanchard, J. S. *Biochemistry* **2004**, *43*, 4375.
(21) Liu, J.; Murkin, A. S. *Biochemistry* **2012**, *51*, 5307.
(22) Erb, T. J.; Brecht, V.; Fuchs, G.; Mueller, M.; Alber, B. E. *Proc. Natl. Acad. Sci. U.S.A.* **2009**, *106*, 8871.
(23) Markham, K. A.; Kohen, A. *Curr. Anal. Chem.* **2006**, *2*, 379.
(24) Kholodar, S. A.; Tombline, G.; Liu, J.; Tan, Z.; Allen, C. L.; Gulick, A. M.; Murkin, A. S. *Biochemistry* **2014**, *53*, 3423.
(25) Kitagawa, M.; Ara, T.; Arifuzzaman, M.; Ioka-Nakamichi, T.; Inamoto, E.; Toyonaga, H.; Mori, H. *DNA Res.* **2005**, *12*, 291.
(26) Hoeffler, J. F.; Tritsch, D.; Grosdemange-Billiard, C.; Rohmer, M. *Eur. J. Biochem.* **2002**, *269*, 4446.
(27) Isobe, K.; Nishise, H. *J. Mol. Catal. B: Enzymol.* **1995**, *1*, 37.
(28) Chan, J.; Lewis, A. R.; Gilbert, M.; Karwaski, M. F.; Bennet, A. J. *Nat. Chem. Biol.* **2010**, *6*, 405.
(29) Manning, K. A.; Sathyamoorthy, B.; Eletsky, A.; Szyperski, T.; Murkin, A. S. *J. Am. Chem. Soc.* **2012**, *134*, 20589.
(30) Bischofberger, N.; Waldmann, H.; Saito, T.; Simon, E. S.; Lees, W.; Bednarski, M. D.; Whitesides, G. M. *J. Org. Chem.* **1988**, *53*, 3457.
(31) Segel, I. H. *Enzyme Kinetics: Behavior and Analysis of Rapid Equilibrium and Steady-State Enzyme Systems*; Wiley-Interscience: New York, 1975.
(32) Hansen, P. E. *Prog. Nucl. Magn. Reson. Spectrosc.* **1988**, *20*, 207.
(33) Duvold, T.; Bravo, J.-M.; Pale-Grosdemange, C.; Rohmer, M. *Tetrahedron Lett.* **1997**, *38*, 4769.
(34) Koppisch, A. T.; Fox, D. T.; Blagg, B. S.; Poulter, C. D. *Biochemistry* **2002**, *41*, 236.
(35) Cleland, W. W. *Biochemistry* **1990**, *29*, 3194.
(36) Cook, P. F.; Cleland, W. W. *Enzyme Kinetics and Mechanism*; Garland Science: New York, 2007.
(37) Streitwieser, A.; Jagow, R. H.; Fahey, R. C.; Suzuki, S. *J. Am. Chem. Soc.* **1958**, *80*, 2326.
(38) Schramm, V. L. *Annu. Rev. Biochem.* **2011**, *80*, 703.
(39) Kholodar, S. A.; Murkin, A. S. *Biochemistry* **2013**, *52*, 2302.
(40) Bjorkelid, C.; Bergfors, T.; Unge, T.; Mowbray, S. L.; Jones, T. A. *Acta Crystallogr. D: Biol. Crystallogr.* **2012**, *68*, 134.
(41) Yajima, S.; Nonaka, T.; Kuzuyama, T.; Seto, H.; Ohsawa, K. *J. Biochem.* **2002**, *131*, 313.
(42) Chen, H.; Zhou, X.; Wang, A.; Zheng, Y.; Gao, Y.; Zhou, J. *Drug Discovery Today* **2015**, *20*, 105.
(43) Barelier, S.; Cummings, J. A.; Rauwerdink, A. M.; Hitchcock, D. S.; Farelli, J. D.; Almo, S. C.; Raushel, F. M.; Allen, K. N.; Shoichet, B. K. *J. Am. Chem. Soc.* **2014**, *136*, 7374.


DOI: 10.1021/ja512911f
*J. Am. Chem. Soc.* 2015, 137, 2748−2756